Thermodynamics of a Protein Acylation: Activation of *Escherichia coli* Hemolysin Toxin†

Lesa M. S. Worsham, Keisha G. Langston, and M. Lou Ernst-Fonberg*

Department of Biochemistry and Molecular Biology, James H. Quillen College of Medicine, Box 70, 581 East Tennessee State University, Johnson City, Tennessee 37614

Received July 16, 2004; Revised Manuscript Received October 5, 2004

ABSTRACT: HlyC, hemolysin-activating lysine-acyltransferase, catalyses the acylation (from acyl−acyl carrier protein [ACP]) of *Escherichia coli* prohemolysin (proHlyA) on the ϵ-amino groups of specific lysine residues, 564 and 690 of the 1024 amino acid primary structure, to form hemolysin (HlyA). Isothermal titration calorimetry was used to measure the thermodynamic properties of the protein acylation of proHlyA-derived structures, altered by substantial deletions and separation of the acylation sites into two different peptides and site directed mutation analyses of acylation sites. Acylation of proHlyA-derived proteins catalyzed by HlyC was overall an exothermic reaction driven by a negative enthalpy. The reaction, whose kinetics are compatible to a ping-pong mechanism, is composed of two partial reactions. The first, the formation of an acyl−HlyC intermediate, was entropically driven, most likely by noncovalent complex formation between acyl-ACP and HlyC; enthalpy-driven acyl transfer followed, resulting in acyl−HlyC and ACPSH product formation. The second partial reaction was an energetically unfavorable acyl transfer from acyl-enzyme intermediate to the final acyl acceptor, a proHlyA derivative. Overall the acylation of proHlyA-derived proteins catalyzed by HlyC was driven by the energetics of the acyl enzyme intermediate reaction. Of the two acylation sites, intactness of the site equivalent to proHlyA K564 was more important for acylation reaction thermodynamic stability.

The plasticity of protein structures and functions is increasingly appreciated. In this vein, fatty acylation of a protein is one way of modifying its biological behavior, sometimes reversibly. For instance, the covalent attachment of fatty acids appears to be important in steering subcellular trafficking of proteins where fatty acylation targets proteins to membrane lipid rafts for subsequent signal transduction (*1*). Moreover, there may be an unexplained specificity inherent in the reaction in that comparably hydrophobic prenyl groups do not substitute for fatty acyl groups as a way of directing proteins to membrane lipid rafts for subsequent signal transduction (*2*). Recently, palmitoylation has been shown to be the switch mechanism in regulation of the visual cycle (*3*). Long-chain fatty acylation of proteins to create acyl proteins is achieved by diverse mechanisms. One class of acyl proteins arises from cotranslational modification by amide linkage of myristic acid to their N-terminal glycine residues (*4*). In another, acylation occurs post-translationally on internal cysteine, threonine, or lysine residues generating S-esters, O-esters, or an amide, respectively (*5*, *6*); compared to N-terminal acylation, these processes are biochemically less understood. Numerous instances of protein internal fatty acylation, generally via thiol esterification of cysteine residues, have been noted (*7*), and palmitoylation of eukaryotic proteins has recently been examined with a view to its reversibility being like phosphorylation−dephosphorylation (*8*). The extent of internal fatty acylation via amide linkage of mammalian proteins is unknown. Acylation of cellular proteins with endogenously synthesized fatty acids in a mouse muscle cell line suggested, however, that at least 30% of protein-bound palmitate was present in amide linkage with undefined residues (*9*).

HlyC, the hemolysin-activating lysine-acyltransferase, which catalyses the internal acylation of *Escherichia coli* prohemolysin (proHlyA)[1] with two fatty acyl groups to form hemolysin (HlyA) is the only internal protein acyltransferase that has been biochemically examined (*10*−*16*). This reaction is remarkable because the behavior of the protein is changed by lipid modification from a benign protein to a toxin. HlyA's toxic function is unequivocally dependent solely upon acylation with no contribution from bacterial lipopolysaccharide or proHlyA (*17*). HlyA toxicity is not restricted to cell lysis; it entrains more subtle but consequential manifestations in infected cells. The launch of biological events by sub-lytic concentrations of HlyA resulting in induction of a second messenger response in host cells that, in turn,

† This work was supported by National Institutes of Health Grants R01-GM62121.

* To whom correspondence should be addressed. Phone: (423) 439-2025. Fax: (423) 439-2030. E-mail: ernstfon@mail.etsu.edu.

[1] Abbreviations used are: proHlyA, *Escherichia coli* hemolysin A protoxin; HlyA, *E. coli* hemolysin A toxin; RTX, repeats in toxin; HlyC, hemolysin-activating lysine-acyltransferase, an acyl-ACP-proHlyA acyltransferase; CyaA, *Bordetella pertusis* RTX toxin; ACP, acyl carrier protein; ACPSH, acyl carrier protein with a free prosthetic group thiol; myristoyl-ACP, acyl carrier protein with a fourteen carbon acyl chain covalently attached to the prosthetic group thiol; acyl-ACP, acyl carrier protein with a long chain fatty acyl covalently attached to the prosthetic group thiol; HEPES, *N*-[2-hydroxyethyl]piperazine-*N*′-[2-ethanesulfonic acid]; SDS, sodium dodecyl sulfate; PAGE, polyacrylamide gel electrophoresis; ITC, isothermal titration calorimetry.

10.1021/bi048479l CCC: $30.25
Published on Web 12/31/2004

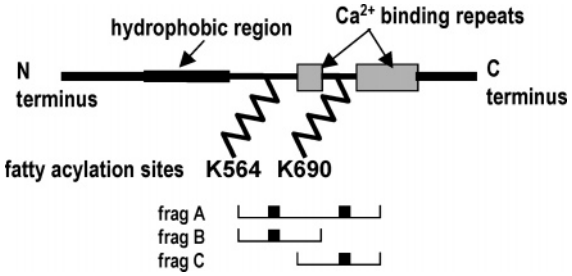

FIGURE 1: Hemolysin structure scheme. Diagram of hemolysin structure showing the acylation sites Lys564 and Lys690 and fragments generated from it, frag A, frag B, and frag C.

results in the induction of inflammation and probably other unidentified cellular events shows the dramatic consequences of the acylation of a protein. Hemolysin is the prototype of the homologous RTX (repeats in toxin) family of toxins secreted by Gram-negative bacteria. RTX toxins arise from the A gene of a CABD operon where the C gene product is the acyltransferase that transfers acyl groups to the A protein (*18*). Acyl-ACP is the obligate acyl donor in *E. coli* (*11*, *16*) where HlyA is acylated on the ϵ-amino groups of lysine residues 564 and 690 of the 1024 amino acid primary structure (*19*). Most other RTX toxins are likely homologously acylated. The identities and functional specificities, if any, of the acyl groups are unresolved in most instances. In vivo acylation of *E. coli* HlyA results in heterogeneous, di-acyl, covalent structures containing saturated fatty acyl groups of 14- (68%), 15- (26%), and 17- (6%) carbon amide-linked side chains, while, in comparison, the acylations observed in RTX toxin from *Bordetella pertussis*, CyaA are highly variable (*20*).

Using separately subcloned, expressed, and purified proteins participating in the acylation of proHlyA to form HlyA, we have previously characterized the acyltransferase HlyC and the reaction it catalyses, the acyl group transfer from acyl-ACP to proHlyA (*11*). The reaction kinetics are consistent with a ping-pong mechanism, and the acyltransfer consists of two partial reactions (*12*, *14*, *15*). As stated above, acylation of proHlyA by HlyC occurs on two precise lysine residues. The substrate specificity of acylation was examined previously using proHlyA-derived structures, altered by substantial deletions and separation of the acylation sites into two different peptides and site-directed mutation analyses of acylation sites (*21*). The abbreviated and/or mutant proteins perform as acylation substrates such as proHlyA's corresponding acylation sites. The two sites of acylation of proHlyA function kinetically independently of one another with HlyC, and acyl-HlyC is likely the enzyme form that interacts with the final acylation substrate. Although the protein acylation catalyzed by HlyC has been characterized mechanistically and kinetically, there is no information regarding the thermodynamics of the reaction or, for that matter, of any reaction resulting in the acylation of a protein. The thermodynamics have been analyzed using isothermal titration calorimetry of the HlyC-catalyzed acylation of the following proHlyA-derived proteins: frag A which contains two acylation sites, and frag C and frag B containing one each of the acylation sites (Figure 1). Similar analyses have been done of the acylation reaction on single site mutants of frag A where one acylation site or the other has been removed by mutation. The thermodynamics of the reaction correlated with the kinetic and chemical mechanisms of the protein acylation.

EXPERIMENTAL PROCEDURES

Expression of Proteins. Proteins were handled at 4 °C unless noted otherwise. Myristoyl-ACP and [1-^{14}C]myristoyl-ACP were prepared as described by Trent and colleagues (*11*). Myristoyl-ACP was purified and evaluated as described (*22*) and stored in aliquots at −80 °C. HlyC, HlyCH23A, and HlyCH23K expressed as His_6−S-tag fusion proteins from pTXC2 and purified as described previously (*11*, *12*) were used for ITC. N-terminal His_6−S-tag fusion frag A, N-terminal His_6−S-tag fusion frag B, and N-terminal His_6−S-tag fusion frag C were expressed and purified from cells grown and induced as previously described (*21*). The generation, expression, and handling of frag A single site mutants K690 and K564 have been described (*21*). Proteins were stored in aliquots at − 80 °C.

Protein Determination. Protein was measured by Bradford's method (*23*) except ACP and its derivatives, which were measured by the bicinchoninic acid protein assay (*24*).

Measurement of Enzyme Activity. The rate at which HlyC catalyzed acyl transfer from [1-^{14}C]myristoyl-ACP to proHlyA or one of its fragments (frag A, frag B, or frag C) was measured as previously described (*11*).

Chemical Cross Linking, Gel Electrophoresis, Western Blotting, and Image Analysis. The purity of each protein used was assessed by densitometry following SDS−PAGE according to Laemmli (*25*); the same technique was used to separate stages in the progress of acyl group movement during acyl-transfer catalyzed by HlyC and its mutants. Coomassie stained gels were scanned using a Hewlet-Packard ScanJet 5200C and analyzed with Un-Scan-It software by Silk Scientific.

To detect heterodimer formation, 100 μL reactions of [1-^{14}C]myristoyl-ACP (10 Ci/M), 1.5 μM, and HlyC, 4.5 μM, in 5 mM Hepes (pH 8.0) were treated with dimethyl suberimidate (10 mM final concentration) in two portions over 20 min. Reaction was halted with 100 mM ammonium acetate. Samples were made 10% with trichloroacetic acid, and, after 45 min on ice, protein was collected by centrifugation at 13 000× *g* for 5 min. Protein pellets were washed with 500 μL cold acetone, collected by centrifugation, dissolved in 20 μL 40 mM TrisHCl (pH 6.8), 8% glycerol, 1% SDS, 6 M urea, and electrophoresed on an SDS-15% PAGE (*25*) that was blotted as described below.

[1-^{14}C]myristoyl-HlyC formation was visualized by incubating [1-^{14}C]myristoyl-ACP (20 Ci/M), 1.8 μM, and HlyC, 9 μM, for 5 min at 20 °C in 100 μL 5 mM Hepes (pH 8.0). The samples were treated with trichloroacetic acid and processed as described.

Frag A acylation was seen upon incubation of [1-^{14}C]-myristoyl-ACP (10 Ci/M), 1.0 μM, frag A, 3 μM, and HlyC, 3.0 μM, in 100 μL 5 mM Hepes (pH 8.0) for 5 min at 20 °C. The reaction was stopped by precipitation with 10% trichloroacetic acid, and the protein pellet was processed as described.

Western blotting onto PVDF membrane (Bio-Rad) was done using a Bio-Rad semi-dry electrophoretic transfer cell according to the manufacturer's instructions. For imaging of [^{14}C] labeled proteins on Western blots, blots were placed

in a BAS-MS 2025 Fujifilm imaging plate cassette then analyzed in a Fujifilm FLA-5000 Science Imaging System equipped with Image Gauge version 3.46 and L Process version 1.96 software.

Isothermal Titration Calorimetry (ITC). Solutions containing myristoyl-ACP and HlyC or HlyC mutants were extensively dialyzed, one protein per dialysis cassette (Pierce), at 4 °C against the same batches of 25 mM Hepes (pH 8.0), and any dilutions or blanks were made with the final dialysis solution. The dialyzed protein solutions were stored in aliquots at −80 °C until use. Frag A, its mutants, frag B, and frag C were not dialyzed; they were put into the calorimeter from concentrated solutions made in 25 mM Hepes (pH 8.0), 1 M dithiothreitol, 5 mM ethylenediamine tetraacetic acid, 6 M urea and kept at −80 °C. Any dilutions were made at the time of the experiment with the final dialysis solution described above. Protein solutions were subjected to a single thawing only. The acyl-acceptor functions of each proHlyA derivative and the catalytic activity of HlyC were unimpaired by preparation for ITC (data not shown).

Isothermal titration calorimetry was performed with an AP−ITC microcalorimeter (MicroCal Inc., Northampton, MA). The principles of experimental design and theory of data anlysis have been described (*26*). The instrument consists of a sample cell, a reference cell, and a spinning syringe immersed in the sample cell. One binding reactant/enzyme is in the sample cell and the other reactant in the spinning syringe. The calorimeter determines the temperature difference between the sample cell and the reference cell. The proteins were titrated by computer-controlled stepwise injections. The change in heating power was followed until equilibrium was reached before the next injection was started. Negative and positive power pulses reflected exothermic and endothermic processes, respectively. Reaction was complete when the heat change leveled off to a constant background value.

Solutions were degassed immediately before use (140 mbar, 10 min). Experiments were performed at 20 °C. A 250 μL injection syringe with 310 rpm stirring was used to perform one 1 μL injection followed by a series of injections of 10 μL at timed intervals of 600 s. The stirred cell contained HlyC (wild-type or mutant) at 1.2 μM and, when it was part of the experiment, frag A or a derivative of it at 3 μM. The syringe contained myristoyl-ACP, 10 μM and, when it was part of the experiment, frag A or a derivative of it, 3 μM. The heat of dilution was quenched relative to the reaction signal by the presence of 10 μM bovine serum albumin in all protein solutions (*27*).

The enthalpy profiles for heat of dilution titrations without HlyC were subtracted from the experimental data sets prior to data analyses. Data acquisition and subsequent nonlinear regression analyses were done in terms of a simple one-site binding model or a two-site sequential model using the Microcal ORIGIN 7 SR2 version 7.0383 software, from which, under appropriate conditions, simultaneous determination of binding parameters K_a (binary equilibrium association constant), $\Delta H°$, $\Delta S°$, and n can be made. ΔG values were calculated from the fundamental equation of thermodynamics: $\Delta G = -RT\ln K_a$ and the standard thermodynamic relationship $\Delta G = \Delta H - T\Delta S$. Each set of proteins was subjected to ITC at least 2−3 different times. Measured

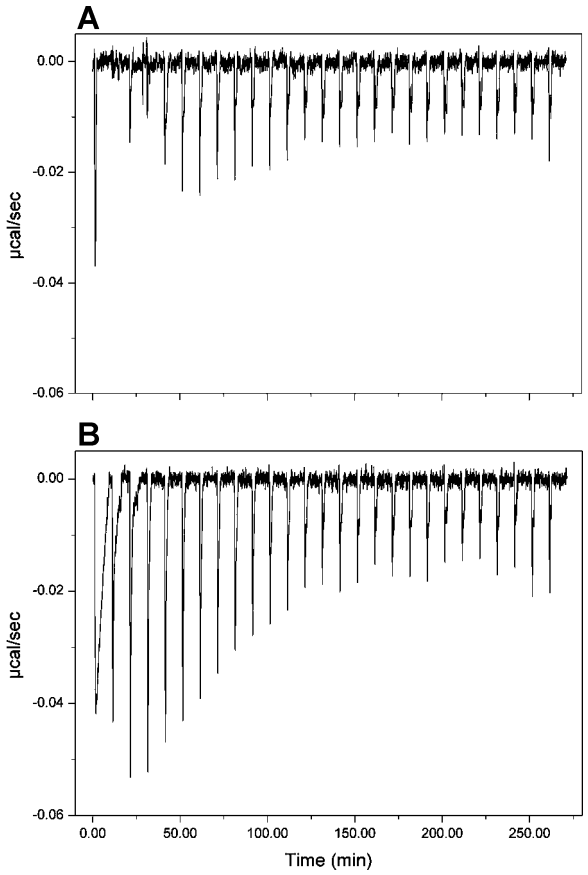

FIGURE 2: Representative raw data showing the heat pulses (in μcal/s) obtained by repetitive injections of frag A and myristoyl-ACP into frag A and HlyC as described in Experimental Procedures. The enzyme HlyC is lacking in A, the blank titration which is, following integration of the areas of the peaks of B, subtracted from the integrated areas of the peak of B prior to nonlinear curve fitting.

thermodynamic values are usually a function of solvent conditions; to indicate this, observed enthalpy and entropy changes herein are abbreviated as ΔH^{obs} and ΔS^{obs} (*28*).

RESULTS

Isothermal Titration Calorimetry of Protein Internal Acylation. The protein acylation catalyzed by HlyC that changes proHlyA into toxic HlyA entails the independent transfer of two fatty acids from thioester linkages with ACPs to specific epsilon amide linkages in HlyA (*20*). Since the solution stability of proHlyA is unreliable (*29*), the thermodynamic properties of internal protein acylation were examined using smaller, more stable, constructs of proHlyA that have been characterized previously (*15*, *21*). ProHlyA's two sites of acylation function independently of one another with HlyC, actually acyl-HlyC (*21*). In a variety of constructs, the acylation sites have similar K_m values, but their V_{max} values and catalytic efficiencies as substrates differ. Frag A acylation kinetics and specificities are like those of proHlyA. The hydrophobic portion of the proHlyA structure has been removed. Frag B and frag C are structures derived from frag A, each containing one unique acylation site (Figure 1). Raw data from an isothermal titration of frag A in the presence of the enzyme HlyC by the acyl-donor myristoyl-ACP is shown in Figure 2B. The negative displacement of the peaks is typical of an exothermic reaction. The apparent increase in peak size at the end of the titration was ignored because

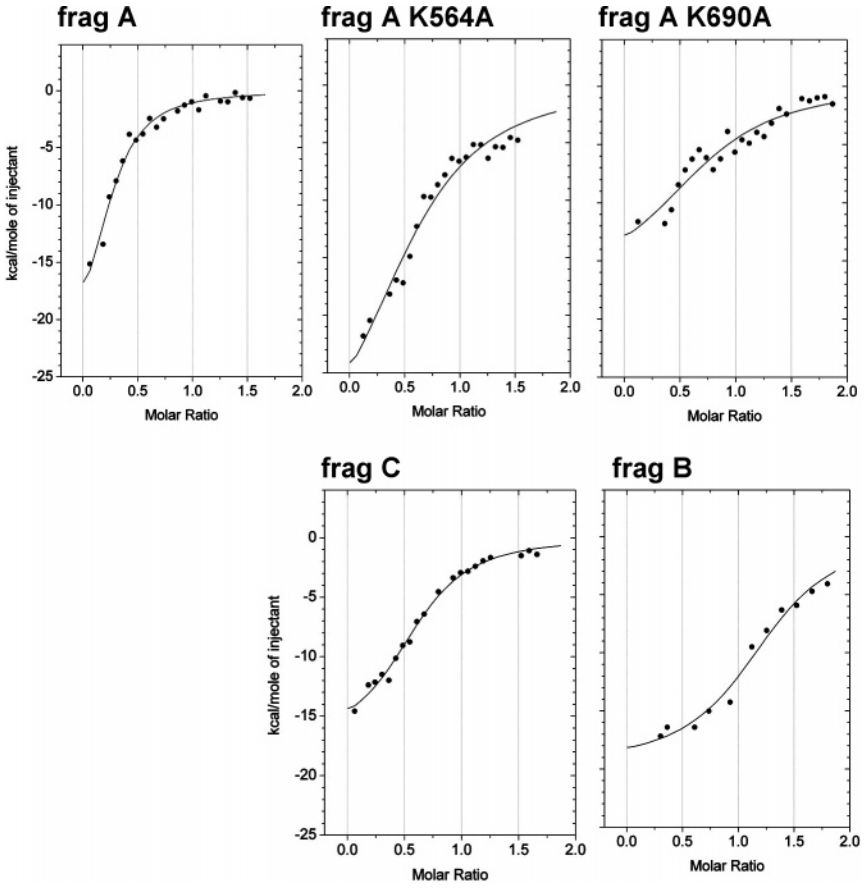

FIGURE 3: Theoretical nonlinear curves fitted using a single-site binding model (solid line) to the blank-corrected integrated areas of the peaks of raw data (solid circles) generated by the internal acylation of the indicated protein derivatives of hemolysin. The internal acylation reaction was catalyzed by HlyC upon titration with the acyl donor myristoyl-ACP. Axes are identical on all plots. Details are given in Experimental Procedures.

Table 1: Thermodynamic Parameters for Acylation of Wild-Type Prohemolysin Toxin Derivative Frag A and Its Variants

reaction	acylation site(s)	ΔH^{obs} kcal/mol	ΔS^{obs} kcal/molK	$T\Delta S^{obs}$ kcal/mol	ΔG^{obs} kcal/mol
frag A + HlyC + myristoyl-ACP	K564	−24.59 ± 2.92	−0.0528	−15.47	−9.12
frag A K564A + HlyC + myristoyl-ACP	K690	−35.55 ± 5.90	−0.0918	−26.90	−8.65
frag A K690A + HlyC + myristoyl-ACP	K564	−20.21 ± 3.57	−0.0400	−11.72	−8.49
frag B + HlyC + myristoyl-ACP	K564	−19.50 ± 1.10	−0.0347	−10.17	−9.33
frag C + HlyC + myristoyl-ACP	K690	−16.64 ± 2.58	−0.0252	−7.384	−9.26

this was observed when the proteins were titrated into buffer for blank correction (Figure 2A) and has been reported by others analyzing the thermodynamic properties of interactions of multiple proteins (*30*). Correction for the heat of dilution came from experiments such as that shown in Figure 2A raw data, where myristoyl-ACP and frag A were titrated into frag A in 25 mM Hepes (pH 8.0). Following integration, the areas of the peaks of the blank were subtracted from the areas of the experimental titration, and the resulting data were subjected to nonlinear curve fitting as described in Experimental Procedures to obtain thermodynamic parameters. ITC analyses of HlyC-catalyzed myristoylation of the following proteins were done: frag A; single site mutants of each of frag A's two acylation site lysine residues, frag A K564A and frag A K690A; frag C, which contains a single acylation site equivalent to that of proHlyA K690; and frag B, which contains a single acylation site equivalent to that of proHlyA K564. Plots of the integrated heat signals from these ITC experiments are shown with identical axes in Figure 3 where the curves varied somewhat among the different myristoylated proteins. The resulting thermodynamic parameters for myristoylation of each of the proteins are in Table 1. K_a values were not reported; they fell between 1 and 9 μM in all reactions. Overall, the reaction myristoylating frag A was driven by a favorable enthalpy change (Table 1). The statistical average ΔG^{obs} and standard deviation for the acylation reaction was −8.97±0.38 kcal/mol for frag A, mutants of either acylation site, and separate protein constructs containing one or the other acylation site, frag B and frag C. Variations in ΔH^{obs} and ΔS^{obs} occurred, however, in response to changes in the acyl acceptor structure. When frag A's more efficient acylation site Lys564 was mutated to an alanine, the ΔH^{obs} of the remaining acylation reaction increased by about −10 kcal/mol from −24.59 kcal/mol to −35.55 kcal/mol while the ΔS^{obs} almost doubled in negativity (Figure 4). When the kinetically more efficient acylation site was removed by creation of a smaller structure, frag C, encompassing only a single acylation site equivalent to

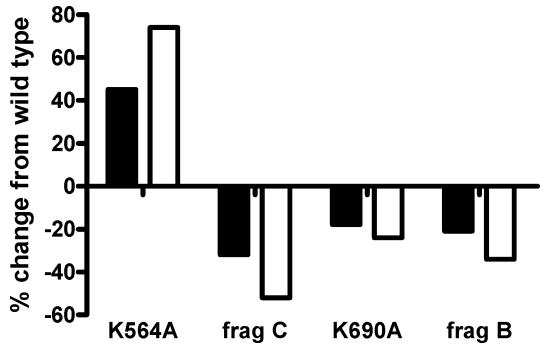

FIGURE 4: Percentage change relative to wild-type in ΔH^{obs} (solid bars) and ΔS^{obs} (clear bars) for internal acylation reaction upon mutation singly of frag A acylation sites or abbreviation of its structure to a single acylation site/peptide. Details are given in Experimental Procedures and thermodynamic parameters in Table 1.

proHlyA Lys690, the negative enthalpy change of the myristoylation reaction decreased and the entropy change became less negative compared to wild-type. In contrast, mutation of the other acylation site of frag A by the single mutation K690A resulted in slightly reduced $-\Delta H^{obs}$ and slightly larger $-\Delta S^{obs}$ of the myristoylation reaction. The smaller structure encompassing the same single acylation site, frag B, showed myristoylation reaction thermodynamics resembling those of frag A K690A. The thermodynamic parameters of myristoylation of the site equivalent to proHlyA K564 were roughly similar whether it was present in frag A or in the smaller peptide frag B. In contrast, the thermodynamic properties of myristoylation of the other acylation site varied depending upon whether it was present in frag A K564A or in frag C, although mutation seemed to evoke a larger effect compared to wild-type than did truncation of the structure.

Component Reactions of the Internal Protein Acylation, Partial Reaction 1. Site-directed mutation analysis of the catalytic mechanism of HlyC and investigation of reaction kinetics indicate that the protein acylation reaction proceeds via a ping-pong mechanism with transient formation of an acyl-HlyC intermediate (*11*−*15*). This mechanism predicts that the reaction is the sum of two partial reactions. The thermodynamic properties of the sum (shown below) or overall reaction were reported above.

Table 2: Thermodynamic Parameters of Partial Reaction 1

reaction	ΔH^{obs} kcal/mol	ΔS^{obs} kcal/molK	$T\Delta S^{obs}$ kcal/mol	ΔG^{obs} kcal/mol
	wild-type HlyC			
HlyC + myristoyl-ACP site 1	151.3 ± 43.9	0.546	160	−8.7
HlyC + myristoyl-ACP site 2	−110.2 ± 41.7	−0.342	−100	−10.2
sum of sites 1 and 2	41.1	0.204	60.0	−18.9
	H23K HlyC			
H23K + myristoyl-ACP site 1	143.5 ± 33.3	0.518	152	−8.5
H23K + myristoyl-ACP site 2	−55.87 ± 34.4	−0.161	−47.2	−8.7
sum of sites 1 and 2	87.63	0.357	105	−17.4
	H23A HlyC			
H23A + myristoyl-ACP	120.7 ± 15.7	0.439	129	−8.3

$$\text{acyl-ACP}+\text{HlyC} \leftrightarrow [\text{HlyC}\cdot\text{acyl-ACP}] \leftrightarrow \text{acyl-HlyC}+\text{ACPSH} \quad (1)$$

$$\underline{\text{acyl-HlyC}+\text{proHlyA} \leftrightarrow [\text{proHlyA}\cdot\text{acyl-HlyC}] \leftrightarrow \text{HlyA}+\text{HlyC}} \quad (2)$$

$$\text{acyl-ACP} + \text{proHlyA} \leftrightarrow \text{HlyA} + \text{ACPSH} \quad \text{(sum)}$$

As we have shown, the first partial reaction is an independent entity (*14*). Its thermodynamic properties were measured in the absence of an ultimate acyl acceptor, a derivative of proHlyA. The data, corrected for heat of dilution, best fitted a nonlinear sequential two-site curve (Figure 5). Partial reaction 1 with an unfavorable enthalpy change of reaction equal to 41.1 kcal/mol was driven by a large positive entropy change factor for the reaction of 60 kcal/mol. This resulted in a relatively high $-\Delta G^{obs}$ of −18.9 kcal/mol (Table 2). The 2 sequential sites components of partial reaction 1, the docking of myristoylACP to HlyC and the actual transfer of the myristoyl group from the ACP to the HlyC with possible conformational change of the acylated enzyme, showed different energetics at each site; the unfavorable ΔH^{obs} of the site 1 was in contrast to a high negative enthalpy change at site 2. The entropy changes of the two sequential sites were opposite in that the first site was positive and the second

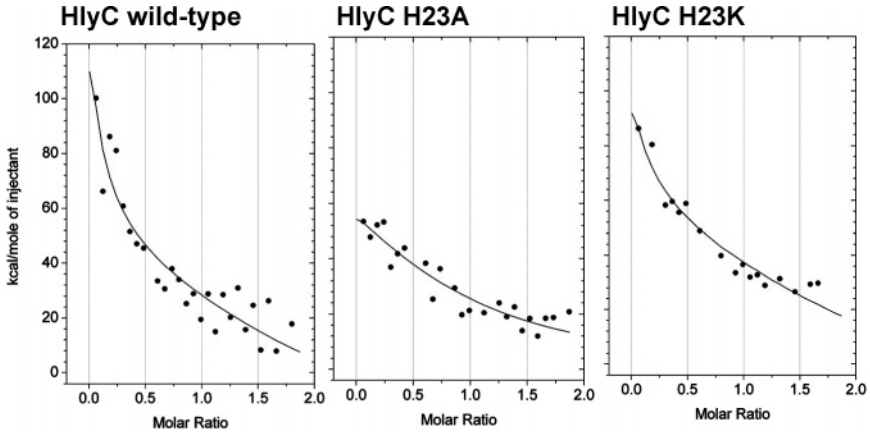

FIGURE 5: Theoretical nonlinear curves fitted using a two-sequential sites binding model (wild-type and H23K) or a single-site binding model (H23A) to the blank-corrected integrated areas of the peaks of raw data (solid circles) generated by the thermal changes upon interaction between HlyC and myristoyl-ACP. This is partial reaction 1 of the internal protein acylation reaction. Details are given in Experimental Procedures.

site was negative. The ΔG^{obs} for each site was roughly similar.

In the acylation reaction, HlyC forms an acyl-enzyme intermediate, most likely at His23 (*12*, *14*, *15*). ITC analyses of partial reaction 1 using a His23 mutant of HlyC, H23A, resulted in data that did not fit a two sequential sites nonlinear curve analysis but fitted a one-site analysis. Curve fitting of the H23A data yielded thermodynamic parameters that resembled those of the wild type sequential site 1 (Table 2). As proposed, this step in the reaction involves the binding of myristoyl-ACP with the enzyme. In contrast, ITC data for a different HlyC acylation site mutant HlyC H23K fitted a two sequential sites nonlinear curve analysis (Figure 5). Thermodynamic parameters of HlyC H23K catalyzed reaction resembled, in part, those of wild-type enzyme, especially the sequential site 1 parameters. The sequential site 2 parameter values were reduced compared to wild-type, possibly indicating the transfer of less myristate from the ACP to the enzyme. The overall result was a less favorable reaction between H23K and myristoyl-ACP, indicated by a more unfavorable enthalpy change with $\Delta H = 87.63$ kcal/mol, compared to 41.1 kcal/mol for wild-type enzyme. The unfavorable enthalpy change was partially compensated for by a positive entropy change, a change that was larger with the H23K mutant than it was with the wild-type enzyme. This, however, was insufficient to prevent a reduction in the $-\Delta G^{obs}$ of 8% for the reaction sum compared to wild-type.

The progress of the transfer of the radiolabeled myristate from [1-^{14}C]myristoyl-ACP to [1-^{14}C]myristoyl-fragA in separated components of the reactions catalyzed by the different His23 mutants of HlyC was limited compared to wild-type (Figure 6). The first step in the reaction, heterodimer (seen at 36 684 Da) formation between HlyC and myristoyl-ACP, was accomplished by all forms of enzyme (Figure 6A), but the next step in the sequence, [1-^{14}C]-myristoyl-HlyC formation (22,594 Da), was not seen with HlyC H23A where the alanine substituted for histidine was unable to be acylated (Figure 6B). Lysine substituted for His23 resulted in an HlyC capable of myristoylation, albeit somewhat reduced compared to wild-type. When an ultimate acyl-acceptor frag A was added to the reaction, only wild-type HlyC catalyzed the formation of [1−14C]myristoyl-fragA (39,543 Da); it can be seen that much of the radiolabeled myristate of the HlyC mutants remained as myristoyl-ACP (Figure 6C). The thermodynamic properties of the reactions catalyzed by wild-type and two mutant His23 HlyCs seemed to correlate with the visible progress of the reaction.

Determination of Thermodynamic Parameters for Partial Reaction 2. Measurement of the thermodynamic parameters for protein acylation of each of the final acyl acceptors (Table 1) and of the thermodynamic parameters for partial reaction 1, common to all acylations catalyzed by HlyC, allowed calculation of the thermodynamic properties of partial reaction 2, unique for each final acyl acceptor (Table 3). For all acyl-acceptors, partial reaction 2 had an unfavorable ΔG^{obs}, roughly 10 kcal/mol. The unfavorable ΔG^{obs} values stemmed from unfavorable entropy changes, large negative $T\Delta S^{obs}$ values compared to smaller negative enthalpy changes. When the site corresponding to K564 was rendered ineffectual for acylation by mutation, the $T\Delta S^{obs}$ of reaction became more negative compared to wild-type. Alternatively,

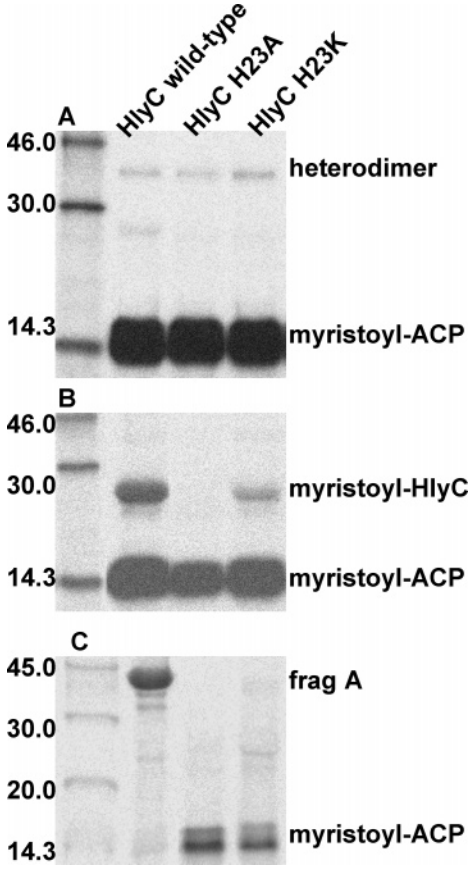

FIGURE 6: Phosphoimage demonstration of the path of the [1-^{14}C]-myristoyl group of [1-^{14}C]myristoyl-ACP, the acyl group donor, during internal protein acylation of fragA catalyzed by HlyC, the acyltransferase, and its His23 mutants. Reaction details are given in Experimental Procedures. Reaction components were separated by SDS-15% PAGE and Western blotted. The myristoyl group was located by phosphoimaging. A. The capabilities of wild-type HlyC and two different HlyC His23 mutants to form a heterodimer with [1-^{14}C]myristoyl-ACP were examined by chemical cross-linking. B. Formation of [1-^{14}C]myristoyl-HlyC using wild-type and His23-mutated HlyCs was examined. C. Formation of [1-^{14}C]myristoyl-frag A catalyzed by wild-type and His23-mutated HlyCs.

Table 3: Calculated Thermodynamic Parameters of Partial Reaction 2

reaction	ΔH^{obs} kcal/mol	ΔS^{obs} kcal/molK	$T\Delta S^{obs}$ kcal/mol	ΔG^{obs} kcal/mol
myristoyl-HlyC + frag A	−65.69	−0.258	−75.47	9.78
myristoyl-HlyC + frag A K564A	−76.65	−0.297	−86.90	10.25
myristoyl-HlyC + frag A K690A	−61.31	−0.230	−71.72	10.41
myristoyl-HlyC + frag B	−60.60	−0.240	−70.17	9.57
myristoyl-HlyC + frag C	−57.74	−0.230	−67.38	9.64

when instead the other site, K690, was removed by mutation, the $T\Delta S^{obs}$ became somewhat less negative than wild-type. Apparently, the overall internal protein acylation reaction was driven by the favorable energetics of partial reaction 1.

DISCUSSION

Frag A and its mutants and frag B and frag C are valid models for protein acylation (*21*). ITC showed that acylation of frag A was driven by the energetics of the acyl-enzyme intermediate formation. The reaction involves the transfer of a myristoyl group from myristoyl-ACP to HlyC, forming the intermediate myristoyl-HlyC. The stability of the acyl-enzyme intermediate is compatible with an acyl histidine,

and His23 of HlyC, a conserved histidine, is essential for catalysis (*12*, *15*). Transfer of the acyl group from myristoyl-HlyC to frag A had a large negative ΔH^{obs} of reaction, which was counteracted by an unfavorable entropy change (Table 3), possibly suggesting constraints in complex formation between myristoyl-HlyC and frag A compared to heterodimer formation between myristoyl-ACP and HlyC. The product inhibition patterns of the acyltransferase reaction kinetics conform to an uni uni iso uni uni ping-pong kinetic mechanism where the acyl enzyme undergoes an isomerization during the course of reaction (*31*); the Cleland notation of the kinetic mechanism of HlyC, acyl-ACP-proHlyA acyltransferase is shown below: F′ and F represent

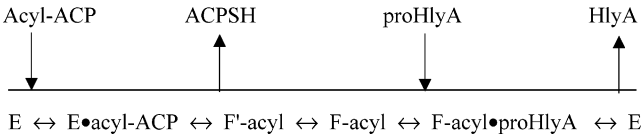

the two isomers of the enzyme. The ITC analyses of partial reaction 1 that fitted a 2 sequential sites nonlinear curve analysis presumably included the wild-type enzyme forms from E through F-acyl. Although possessing an unfavorable enthalpy change, the first part of the reaction (Table 2, site 1) was driven by a large positive entropy change factor, likely derived from complex formation between HlyC and myristoyl-ACP. We, using site-directed fluorescence probes, have previously mapped HlyC complex formation with myristoyl-ACP to be spread over one face of myristoyl-ACP with contacts distributed around the covalent binding region on the S-atom on the prosthetic group of ACP, thus advantageously positioning the acyltranferase for catalysis (*32*). A positive ΔS factor is a solid indication that water molecules have been expelled from the interface during complex formation (*33*). Subsequent transfer of the myristoyl group from ACP to HlyC culminating in the formation of ACPSH, the first product, and myristoyl-HlyC had a large negative change in enthalpy and an unfavorable entropy change factor (Table 2, site 2). Part of the large negative enthalpy change likely stemmed from the transfer of the energy of the thiolester bond of myristoyl-ACP to myristoyl-HlyC. ACPSH was released from the noncovalently bound bi-macromolecular complex. In the progress of the reaction, it went from the more structured protein myristoyl-ACP to the comparatively less structured protein ACPSH. The negative entropy change of the release of ACPSH came, at least partly, from the hydration of polar and apolar groups accompanying the increase of water accessible surface within its relatively open structure. As pointed out previously (*32*), ACPSH is likely one of the intrinsically unstructured proteins whose conformations are shaped through interactions with other macromolecules, a feature consistent with its ability to recognize assorted targets in its myriad of biological functions (*32*, *34*−*36*). This view stems, partly, from the following observations: ACP's heat stable structure that long resisted crystallization has been shown to contain an unusually mobile combination of ordered and disordered helices in its solution structure that is best represented as an equilibrium of multiple conformers (*37*, *38*). Highly mobile portions include the loop regions and helix II (*38*), regions important in interactions with other proteins (*32*, *40*). ACPs from diverse sources exhibit intrinsic plasticity of structure shown, for example, by the NMR solution structure of *Mycobacterium tuberculosis* (*41*). Thus, large entropy changes may be anticipated as ACP associates and dissociates with other macromolecules; similar fluctuations in thermodynamic properties have been shown for other interactive intrinsically disordered proteins (*42*).

HlyC mutants impaired to differing extents in acyltransfer support the above interpretation of the partial reaction 1 events and their associated thermodynamic characteristics. HlyC H23A, where the presumed histidine nucleophile is mutated to an alanine, was unable to form the myristoyl-HlyC intermediate essential for reaction, but it formed the heterodimer with myristoyl-ACP, the first step in the progression to myristoyl-HlyC (Figure 6). HlyC H23A had thermodynamic parameters similar to those of the first portion of partial reaction 1, site 1 of the nonlinear sequential 2 sites curve of the wild-type HlyC catalyzed reaction. This finding supported the conjecture that site 1 interaction involved noncovalent binding between enzyme and acyl-donor to form a heterocomplex. In contrast, data from reaction between myristoyl-ACP and HlyC H23K, which formed myristoyl-HlyC but did not transfer the acyl group to complete the reaction, fitted the 2 sequential sites nonlinear curve analysis. The amide bond formed by nucleophilic attack by the lysine of the H23K mutant would be less reactive than the myristoyl−histidine bond of wild-type HlyC. Acyl imidazole is thermodynamically unstable compared with most amides, esters, and thiol esters (*43*). HlyC H23K site 1 thermodynamic parameters were like those of wild-type, but its site 2 thermodynamic parameters were reduced compared to wild-type (Table 2). The ΔG^{obs} for H23K site 2 reaction was 15% less favorable than that of wild-type. Such a large change in ΔG upon mutation supports previous evidence that His23 is a highly significant residue in HlyC catalysis (*12*, *14*, *15*).

Partial reaction 1 was common to all ultimate acyl acceptors. Any mutations or structural deletions of ultimate acyl acceptors would affect exclusively the thermodynamics of partial reaction 2, and, of course, its contribution to the overall reaction.

The entropy change in partial reaction 2 was not favorable (Table 3). This was in marked contrast to partial reaction 1 where favorable entropy change likely stemmed from macromolecular complex formation between myristoyl-ACP and HlyC; perhaps the contrast between the entropy change properties of the two partial reactions lay in the differences between binding of a relatively unstructured protein such as myristoyl-ACP compared with binding of a structured protein like myristoyl-HlyC. Since the latter is an enzyme, it is expected to have a well-defined structure (*35*). Although the second partial reaction had a large negative enthalpy change, it had a free energy of reaction of 9.78 kcal/mol, which was unfavorable. Internal acylation of frag A was not a facile event. The overall reaction demonstrated the energetic advantage of the formation of an acyl enzyme reactive intermediate to drive acylation of internal residues of a protein where the ΔG^{obs} of the global event was −9.12 kcal/mol.

Entropy−enthalpy compensation effects on ΔG^{obs}, where large variations in ΔS^{obs} and ΔH^{obs} appear to be correlated in such a way as almost to cancel and give correspondingly smaller changes in ΔG^{obs} (*45*, *46*), largely obscured the effects of mutation or structural deletion on the ultimate acyl

acceptor. This is evident in Table 3 where the substrates for acylation were subjected to mutation or structural deletion, yet the average ΔG^{obs} and standard deviation for all structures was 9.93±0.38. In contrast to this small standard deviation, similar averages of the entropy factor, $T\Delta S^{obs}$, and ΔH^{obs} were 74.33±7.6 and 64.40±7.42, respectively. Thermodynamic stability appears to be inherent in biological systems and is served by entropy−enthalpy compensation effects that override effects on ΔG except for crucial locations or "hot spots" such as was pointed out above for HlyC His23 residue in partial reaction 1 (*46*). The acyl substrate experimental manipulation that most perturbed thermodynamic parameters was removal of the acylation site equivalent to proHlyA K564 by mutation or deletion (Table 1). This is obvious in Figure 4 where mutation frag A K564A showed 45% and 74% increases in ΔH^{obs} and $T\Delta S^{obs}$, respectively. Frag C, which also has a single acylation site equivalent to proHlyA K690, showed large but opposite changes in the same parameters. So removal of the acylation site equivalent to proHlyA K564 somehow affected the thermodynamic properties of the reaction at the remaining site. Removal of the other acylation site, equivalent to proHlyA K690, produced less dramatic thermodynamic changes that were similar regardless of the way that the site was removed (Figure 4 and Table 1). Thus integrity of the acylation site equivalent to proHlyA K564 appeared to be more important for acylation reaction thermodynamic stability; this is also the kinetically more active of the two sites (*21*).

There is a precedent that alteration at one acylation site affects aspects of protein acylation at the other site. *B. pertusis* RTX toxin CyA is activated by a single acylation at Lys983 that corresponds in sequence homology to the second *E. coli* proHlyA site, Lys690 (*40*). The biological activity of the CyaA toxin that is monoacylated at Lys983, nevertheless, requires the integrity of Lys860, the lysine residue that corresponds to the Lys564 acylation site of HlyA (*40*, *41*). In contrast, HlyA is acylated at two sites with Lys564 being the more efficient site. The two acylation sites in the *E. coli* hemolysin system function independently of one another in the kinetics of their interaction with HlyC, actually acyl-HlyC (*21*). But here we observed that loss of the equivalent of proHlyA Lys564 acylation site either by mutation or structural deletion affected the thermodynamics of the acylation reaction at the site corresponding to proHlyA Lys690, implying an undefined connectivity between the acylation sites in HlyA as well as CyaA.

In conclusion, internal protein acylation at two specific sites of proHlyA-derived proteins catalyzed by HlyC is overall an exothermic reaction driven by a negative enthalpy. The reaction is composed of two partial reactions, the first of which is the formation of an acyl-HlyC intermediate that is entropically driven most likely by noncovalent complex formation between acyl ACP and HlyC. Enthalpy-driven acyl transfer follows this, resulting in acyl HlyC and ACPSH product formation. The second partial reaction was an energetically unfavorable acyl transfer from acyl-enzyme intermediate to the final acyl acceptor, a proHlyA derivative. Overall the internal acylation of proHlyA-derived proteins catalyzed by HlyC was driven by the energetics of the acyl-enzyme intermediate reaction. Intactness of acylation site equivalent to proHlyA K564 appeared to be more important for acylation reaction thermodynamic stability. Loss of the equivalent of proHlyA Lys564 acylation site either by mutation or structural deletion affected the thermodynamics of the acylation reaction at the site corresponding to proHlyA Lys690, implying an undefined connectivity between the acylation sites in HlyA that was not evident in their function as acylation substrates (*21*).

REFERENCES

1. Melkonian, K. A., Ostermeyer, A., Chen, J. Z., Roth, M., and Brown, D. A. (1999) Role of lipid modifications in targeting proteins to detergent-resistant membrane rafts, *J. Biol. Chem. 274*, 3910−3917.
2. Arni, S., Keilbaugh, S. A., Ostermeyer, A., and Brown, D. A. (1998) Association of GAP-43 with detergent- resistant membranes requires two palmitoylated cysteine residues, *J. Biol. Chem. 273*, 28478−28485.
3. Xue, L., Gollapalli, C. R., Maiti, P., Jahng, W. J., and Rando, R. R. (2004) A palmitoylation switch mechanism in the regulation of the visual cycle, *Cell 117*, 761−771.
4. Farazi, T. A., Waksman, G., and Gordon, J. I. (2001) The biology and enzymology of protein *N*-myristoylation, *J. Biol. Chem. 276*, 39501−8650.
5. Hedo, J. A., Collier, C., and Watkinson, A. (1987) Myristoyl and palmitoyl acylation of the insulin receptor, *J. Biol. Chem. 262*, 954−957.
6. James, G., and Olson, E. N. (1990) Fatty acylated proteins as components of intracellular signaling pathways, *Biochemistry 29*, 2624−2634.
7. Bhatnagar, R. S., and Gordon, J. I. (1997) Understanding covalent modifications of protein by lipids: Where cell biology and biophysics mingle, *Trends Cell Biol. 7*, 14−20.
8. Linder, M. E., and Deschenes, R. J. (2003) New insights into the mechanisms of protein palmitoylation, *Biochemistry 42*, 4311−4320.
9. Towler, D., and Glaser, L. (1986) Acylation of cellular proteins with endogenously synthesized fatty acids, *Biochemistry 25*, 878−884.
10. Nicaud, J. M., Mackman, N., Gray, L., and Holland, I. B. (1985) Characterization of HlyC and mechanism of activation and secretion of hemolysin from *E. coli* 2001, *FEBS Lett. 187*, 339−344.
11. Trent, M. S., Worsham, L., and Ernst-Fonberg, M. L. (1998) The biochemistry of hemolysin toxin activation: Characterization of HlyC, an internal protein acyltransferase, *Biochemistry 37*, 4644−4652.
12. Trent, M. S., Worsham, L., and Ernst-Fonberg, M. L. (1999) HlyC, the internal protein acyltransferase that activates hemolysin toxin: Role of conserved histidine, serine, and cysteine residues in enzymatic activity as probed by chemical modification and site-directed mutagenesis, *Biochemistry 38*, 3433−3439.
13. Trent, M. S., Worsham, L., and Ernst-Fonberg, M. L. (1999) HlyC, the internal protein acyltransferase that activates hemolysin toxin: The role of conserved tyrosine and arginine residues in enzymatic activity as probed by chemical modification and site-directed mutagenesis, *Biochemistry 38*, 8831−8838.
14. Trent, M. S., Worsham, L., and Ernst-Fonberg, M. L. (1999) HlyC, the internal protein acyltransferase that activates hemolysin toxin: Roles of various conserved residues in enzymatic activity as probed by site-directed mutagenesis, *Biochemistry 38*, 9541−9548.
15. Worsham, L., Trent, M. S., Earls, L., Jolly, C., and Ernst-Fonberg, M. L. (2001) Insights into the catalytic mechanism of HlyC, the internal protein acyltransferase that activates *Escherichia coli* hemolysin toxin, *Biochemistry 40*, 13607−13616.
16. Stanley, P., Packman, L., Koronakis, V., and Hughes, C. (1994) Fatty acylation of two internal lysine residues required for the toxin activity of *Escherichia coli* hemolysin, *Science 266*, 1992−1996.
17. Uhlen, P., Laestadius, A., Jahnukainen, T., Söderblom, T., Bäckhed, F., Celsi, G., Brismar, H., Normark, S., Aperia, A., and Richter-Dahlfors, A. (2000) α-Haemolysin of uropathogenic *E. coli* induces Ca^{2+} oscillations in renal epithelial cells, *Nature 405*, 694−697.
18. Welch, R. A. (2001) RTX toxin structure and function: A story of numerous anomalies and few analogies in toxin biology, *Curr. Top. Microbiol. Immunol. 257*, 85−111.

19. Ludwig, A., Garcia, F., Bauer, S., Jarchau, T., Benz, R., Hoppe, J., and Goebel, W. (1996) Analysis of the in vivo activation of hemolysin (HlyA) from *Escherichia coli*, *J. Bacteriol. 178*, 5422−5430.
20. Lim, K. G., Walker, C. R. B., Guo, L., Pellett, S., Shabanowitz, J., Hunt, D. F., Hewlett, E. L., Ludwig, A., Goebel, W., Welch, R. A., and Hackett, M. (2000) *Escherichia coli* α-hemolysin (HlyA) is heterogeneously acylated in vivo with 14-, 15-, and 17-carbon fatty acids, *J. Biol. Chem. 275*, 36698−36702.
21. Langston, K. G., Worsham, L., Earls, L., and Ernst-Fonberg, M. L. (2004) Activation of hemolysin toxin: Relationship between two internal protein sites of acylation, *Biochemistry 43*, 4338−4346.
22. Worsham, L., Williams, S., and Ernst-Fonberg, M. L. (1993) Early catalytic steps of *Euglena gracilis* choroplast type II fatty acid synthase, *Biochim. Biophys. Acta 1170*, 62−71.
23. Bradford, M. M. (1976) A rapid and sensitive method for the quantitation of microgram quantities of protein utilizing the principle of protein-dye binding, *Anal. Biochem. 72*, 748−754.
24. Brown, R. E., Jarvis, K. L., and Hyland, K. J. (1989) Protein measurement using bicinchoninic acid: Elimination of interfering substances, *Anal. Biochem. 180*, 136−139.
25. Laemmli, V. (1970) Cleavage of structural proteins during the assembly of the head of bacteriophage T4, *Nature 227*, 680−685.
26. Wiseman, T., Williston, S., Brandts, J., and Lin, L.-N. (1989) Rapid measurement of binding constants and heats of binding using a new titration calorimeter, *Anal. Biochem. 179*, 131−137.
27. Williams, B. A., and Toone, E. J. (1993) Calorimetric evaluation of enzyme kinetic parameters, *J. Org. Chem. 58*, 3507−3510.
28. Fasolini, M., Wu., X., Flocco, M., Trosset, J., Oppermann, U., and Knapp, S. (2003) Hot spots in Tcf4 for the interaction with β-catenin, *J. Biol. Chem. 278*, 21092−21098.
29. Soloaga, A., Ramírez, J., and Goñi, F. M. (1998) Reversible denaturation, self-aggregation, and membrane activity of *Escherichia coli* α-hemolysin, a protein stable in 6 M urea, *Biochemistry 37*, 6387−6393.
30. Crump, M. P., Ceska, T. A., Spyracopoulos, L., Henry, A., Archibald, S., Alexander, R., Taylor, R., Findlow, S., O'Connell, J., Robinson, M., and Shock, A. (2004) Structure of an allosteric inhibitor of LFA-1 bound to the I-domain studied by crystallography, NMR, and calorimetry, *Biochemistry 43*, 2394−2404.
31. Trent, M. S. (1998) Biochemistry of hemolysin toxin activation by fatty acylation: Characterization of an internal protein acyltransferase; Ph.D. Dissertation East Tennessee State University.
32. Worsham, L., Earl, L., Jolly, C., Langston, K. G., Trent, M. S., and Ernst-Fonberg, M. L. (2003) Amino acid residues of *Escherichia coli* acyl carrier protein involved in heterologous protein interactions, *Biochemistry 42*, 167−176.
33. Jelesarov, I., and Bosshard, H. R. (1999) Isothermal titration calorimetry and differential scanning calorimetry as complementary tools to investigate the energetics of biomolecular recognition, *J. Mol. Recognit. 12*, 3−18.
34. Wright, P. E., and Dyson, H. J. (1999) Intrinsically unstructured proteins: re-assessing the protein structure−function paradigm, *J. Mol. Biol. 293*, 321−331.
35. Tompa, P. (2002) Intrinsically unstructured proteins, *TRENDS Biochem. Sci. 27*, 527−533.
36. Dunker, A. K., Brown, C. J., Lawson, J. D., Iakoucheva, L. M., and Obrandović, Z. (2002) Intrinsic disorder and protein function, *Biochemistry 41*, 6573−6582.
37. Kim, Y., and Prestegard, J. H. (1989) A dynamic model for the structure of acyl carrier protein in solution, *Biochemistry 28*, 8792−8797.
38. Ernst-Fonberg, M. L., Worsham, L. M. S., and Williams, S. G. Comparison of acyl-carrier protein and other protein structures in aqueous solutions by Fourier-transform infrared spectroscopy, *Biochim. Biophys. Acta 1164*, 273−282.
39. Andrec, M. R., Hill, R. B., and Prestegard, J. H. (1995) Amide exchange rates in *Escherichia coli* acyl carrier protein: Correlation with protein structure and dynamics, *Protein Science 4*, 983−993.
40. Zhang, Y.-M., Rao, M. S., Heath, R. J., Price, A. C., Olson, A. J., Rock, C. O., and White, S. W. (2001) Identification and analysis of the acyl carrier protein (ACP) docking site on β-ketoacyl-ACP synthase III, *J. Biol. Chem. 276*, 8231−8238.
41. Wong, H. C., Liu, G., Zhang, Y.-M., Rock, C. O., and Zheng, J. (2002) The solution structure of acyl carrier protein from *Mycobacterium tuberculosis*, *J. Biol. Chem. 277*, 15874−15880.
42. Lacy, E. R., Filippov, I., Lewis, W. S., Otieno, S., Xiao, L., Weiss, S., Hengst, L., and Kriwacki, R. W. (2004) p27 binds cyclin-CDK complexes through a sequential mechanism involving binding-induced protein folding, *Nature Struct. Biol. 11*, 358−364.
43. Jencks, W. P. (1969) *Catalysis in Chemistry and Enzymology*, pp. 67−71, McGraw-Hill, New York.
44. Cooper, A. (1999) Thermodynamic analysis of biomolecular interactions, *Curr. Opinion Chem. Biol. 3*, 557−563.
45. Cooper, A., Johnson, C., Lakey, J., and Nöllmann, M. (2001) Heat does not come in different colours: entropy-enthalpy compensation, free energy windows, quantum confinement, pressure perturbation calorimetry, solvation and the multiple causes of heat capacity effects in biomolecular interations, *Biophys. Chem. 93*, 215−230.
46. Basar, T., Havlíček, V., Bezoušková, S., Hackett, E. L., and Šebo, P. (2001) Acylation of lysine 983 is sufficient for toxin activity of *Bordetella pertussis* adenylate cyclase, *J. Biol. Chem. 276*, 348−354.
47. Basar, T., Havlíček, V., Bezušková, S., Halada, P., Hackett, M., and Šebo, P. (1999) The conserved lysine 860 in the additional fatty-acylation site of *Bordetella pertussis* adenylate cyclase is crucial for toxin function independently of its acylation status, *J. Biol. Chem. 274*, 10777−10783.

BI048479L